Electronic Supplementary Material (ESI) for Nanoscale.


# Supplementary Information: Ultrafast Carrier Dynamics and Layer-Dependent Carrier Recombination Rate in InSe

*Ting-Hsuan Wu,* [a,b] *Hao-Yu Cheng,* [a,b,c] *Wei-Chiao Lai,* [a] *Raman Sankar,* [a]

*Chia-Seng Chang* *[a,b] *and Kung-Hsuan Lin* *[a]

[a] Institute of Physics, Academia Sinica, Taipei 11529, Taiwan.

[b] Department of Physics, National Taiwan University, Taipei 10617, Taiwan.

[c] Nano-Science and Technology Program, Taiwan International Graduate Program, Academia Sinica, Taipei 115201, Taiwan.

*Email of Corresponding authors: jasonc@phys.sinica.edu.tw (C.-C. Chang);

linkh@sinica.edu.tw (K.-H. Lin).

## S1: Absorption and photoluminescence (PL) measurement

In order to identify the A-exciton transition and the bandgap of InSe flakes, we performed absorption and PL measurements at room temperature. In the PL measurement, InSe sample was excited by a continuous-wave laser at the wavelength of 532 nm. As shown by the red line in Fig. S1(a), the peak of PL spectrum at ~1.241 eV reflects the bandgap energy. In the absorption measurement, the transmission spectra of InSe samples were measured by using a home-built setup with a micron-sized optical spot. The absorption coefficient $\alpha$, determined from Beer-Lambert law[1], is shown by the black line in Fig. S1(a). We further fitted the spectrum near the band edge, according to Elliott's formula[2-4]:

$$\alpha(\hbar\omega) = A \cdot \theta\left(\hbar\omega - E_{\mathrm{g}}\right) \cdot \left(\frac{1}{1-\exp(-2\pi x)}\right) + A \cdot \sum_{n_{\mathrm{ex}}=1}^{\infty} \frac{2R_{\mathrm{ex}}}{n_{\mathrm{ex}}^3} \cdot \delta\left(\hbar\omega - E_{\mathrm{g}} + R_{\mathrm{ex}}/n_{\mathrm{ex}}^2\right),$$

where $A$ is the normalization constant, $\theta$ is the step function convolved with the Gaussian broadening function with the standard deviation $\sigma_{\mathrm{c}}$, $\omega$ is the frequency of light, $E_{\mathrm{g}}$ is the intrinsic bandgap, $x$ is defined as $R_{\mathrm{ex}}^{1/2}/\left(\hbar\omega - E_{\mathrm{g}}\right)^{1/2}$ where $R_{\mathrm{ex}}$ is the exciton binding energy, $n_{\mathrm{ex}}$ is the principal quantum number and $\delta$ is the delta function convolved with the Gaussian broadening function with the standard deviation $\sigma_{\mathrm{ex}}$. The first term describes the continuum absorption, and the second term is for the exciton absorption. We set the excitonic transitions with $n_{\mathrm{ex}}$ only to 6 because the oscillator strength would decrease as $1/n_{\mathrm{ex}}^3$. The fitting traces are shown in Fig. S1(b). We found the best-fit values of $E_{\mathrm{g}}$, $R_{\mathrm{ex}}$, $\sigma_{\mathrm{c}}$ and $\sigma_{\mathrm{ex}}$ to be 1.239 ± 0.004 eV, 10.0 ± 0.7 meV, 29.0 ± 0.9 meV and 29.0 ± 0.5 meV, respectively. From the PL and absorption measurements, the bandgap was determined to be 1.24 eV at room temperature, which agrees with previous reports[2, 5, 6].

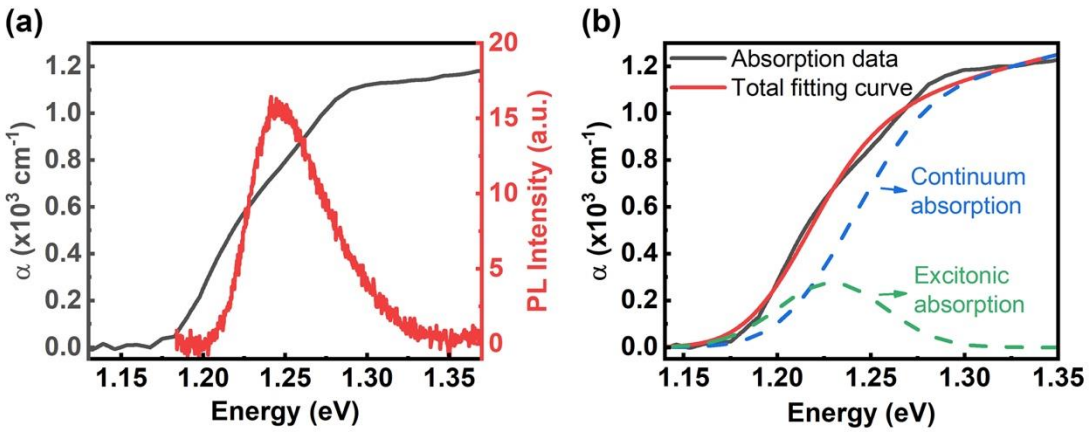


**Figure S1.** Absorption and PL spectra of InSe. (a) Absorption coefficient (in black line) and PL (in red line) spectra at room temperature. (b) Fitted absorption coefficient spectra (in red line) to the experimental result (in black line). The green and blue lines depict the excitonic and free-carrier continuum components in the Elliott's formula.

## S2: Experimental details of hot carrier dynamics

Ti:sapphire ultrafast laser system was utilized to perform pump-probe reflection spectroscopy. The repetition rate was 80 MHz and the central energy ranged from 1.20 to 1.38 eV. The pump beam was frequency-doubled with a beta barium borate (BBO) crystal and modulated with an acousto-optical modulator (AOM) at 100 kHz. The probe beam was directed through a motorized delay stage for controlling the time delay between the pump and probe pulses. The pump and probe beams were recombined collinearly with a dichroic mirror (DMLP650, Thorlabs). The collinear pump/probe beams were focused onto the samples with a long working distance 20X objective lens (NA 0.35, Olympus). The full-width-at-half-maximum (FWHM) of the focused spot was ~5 μm. An optical filter (FGL610, Thorlabs) was utilized to block the reflected pump beam, and the reflected probe beam was sensed by a photodetector (DFT100A/M, Thorlabs). The photocurrent signals were demodulated with a lock-in amplifier (SR844, Stanford Research Systems) to extract the signal $\Delta R$. The signal was divided by R, which was obtained by modulating the probe beam in the absence of pump beam. The duration of the cross-correlation of pump/probe beams was ~600 fs.

For the pump-probe measurements with high spectral resolution of probe energy, the probe pulse (with FWHM bandwidth of ~ 20 nm) was sent to a monochromator (SpectraPro-2500i, Acton) to resolve the spectral responses with a bandwidth of ~1 nm. After the monochromator, a photomultiplier (PMT) (R5108, Hamamatsu) was used to detect the reflection changes of the probe light.

## S3: Experimental data of hot carrier dynamics

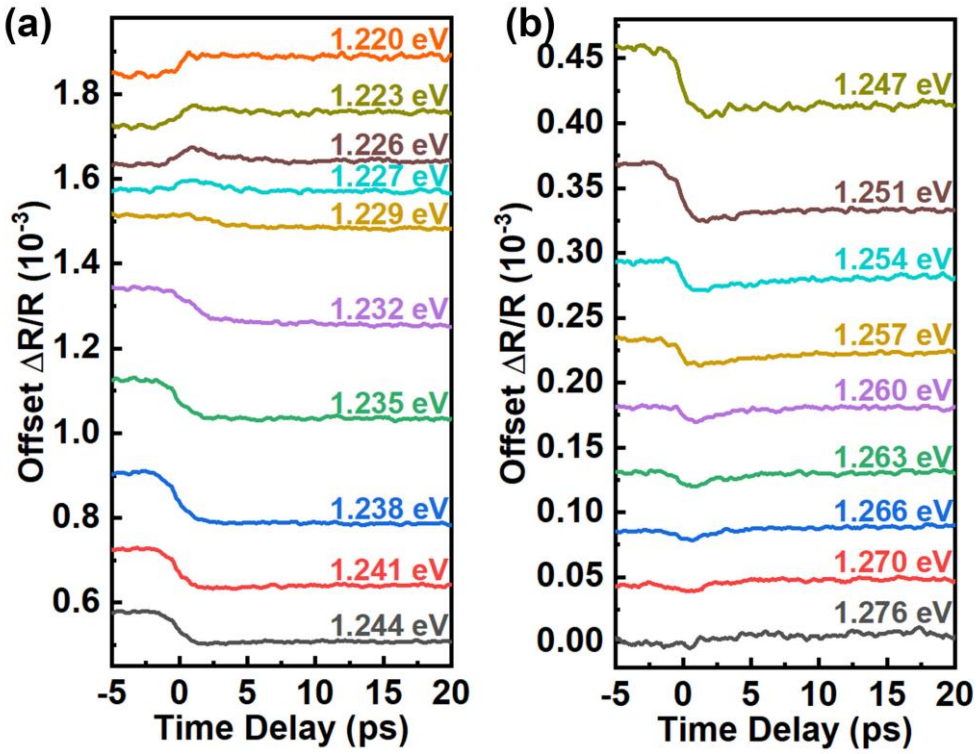


**Figure S2.** Time-resolved reflectivity changes for probe energies (a) from 1.220 eV to 1.244 eV, and (b) from 1.247 eV to 1.276 eV. The central energy of the pump pulses is 2.48 eV.

## S4: Experimental details of layer-dependent carrier recombination dynamics

The experimental setup of ultrafast pump-probe micro-spectroscopy is similar to that in Ref. 7. The central energy of pump and probe pulse is 1.58 eV and 1.61 eV, respectively. The duration of cross correlation between pump and probe pulses was ~1 ps. In this work, a long working distance 50X objective lens (NA 0.5, Olympus) was used instead. The FWHM of the optical spot on the samples was ~1 μm. The samples were in a vacuum box which was mounted on an inverted optical microscope (IX83, Olympus).

## S5: Determination of thickness by a tapping mode atomic force microscopy (AFM)

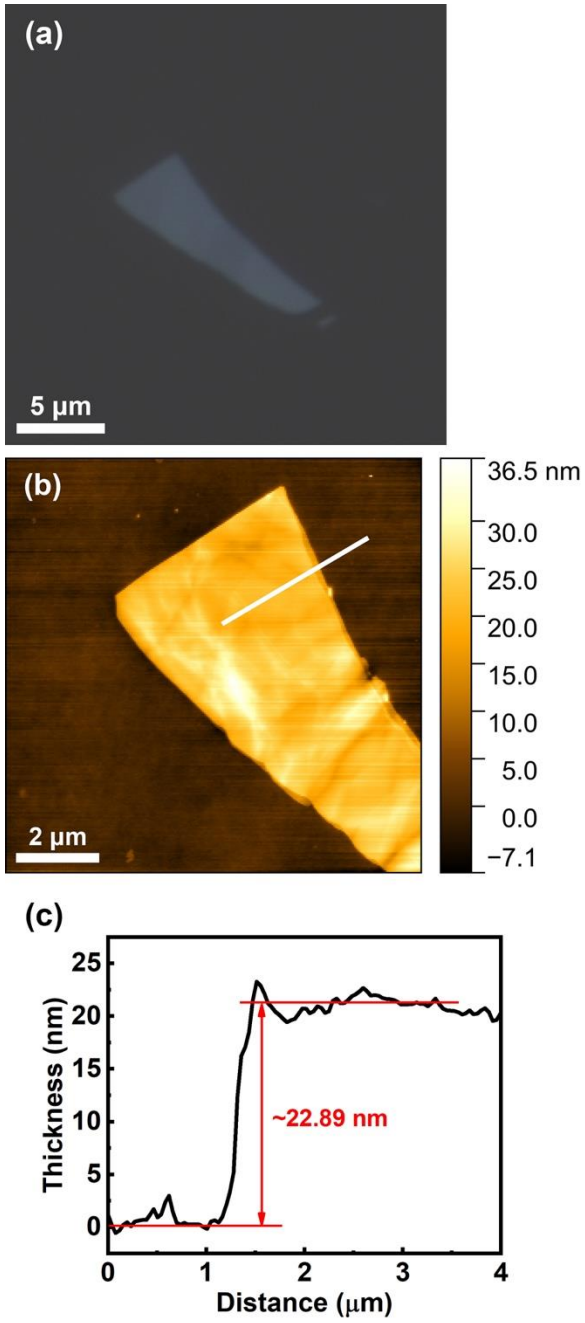


**Figure S3.** Morphology of InSe nanoflake on PDMS. (a) Optical image. (b) AFM image. (c) Height profile of white solid line in (b).

## S6: Carrier recombination probe at two different photon energies

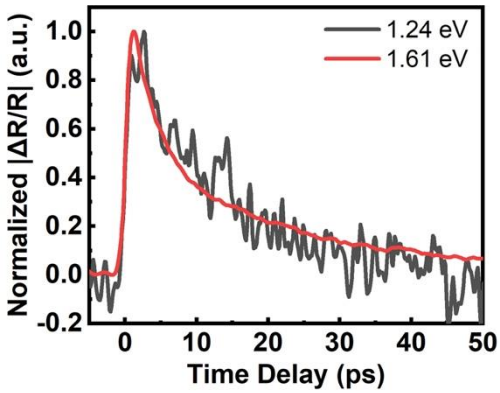


**Figure S4.** Normalized pump-probe curves of InSe at the probe energy of 1.24 eV and 1.61 eV, respectively. The pump energy is 1.58 eV for both cases. Both curves are overlapped with each other, revealing the same carrier recombination process probed by different energies.

## S7: Fluence-dependent measurements

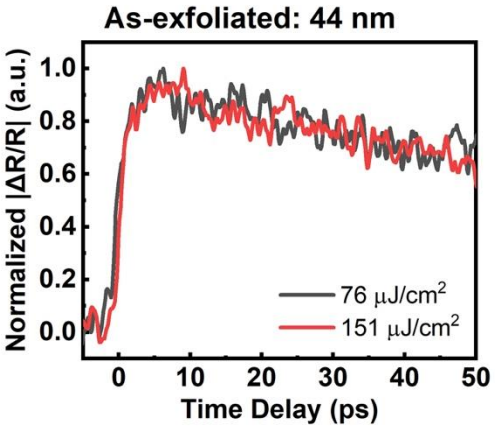


**Figure S5.** Normalized pump-probe curves of InSe under the pump fluences of 76 μJ/cm and 151 μJ/cm, respectively. Both curves are overlapped with each other, revealing no dependence of carrier density on the carrier recombination time.

## S8: Fitting results based on a free carrier diffusion model

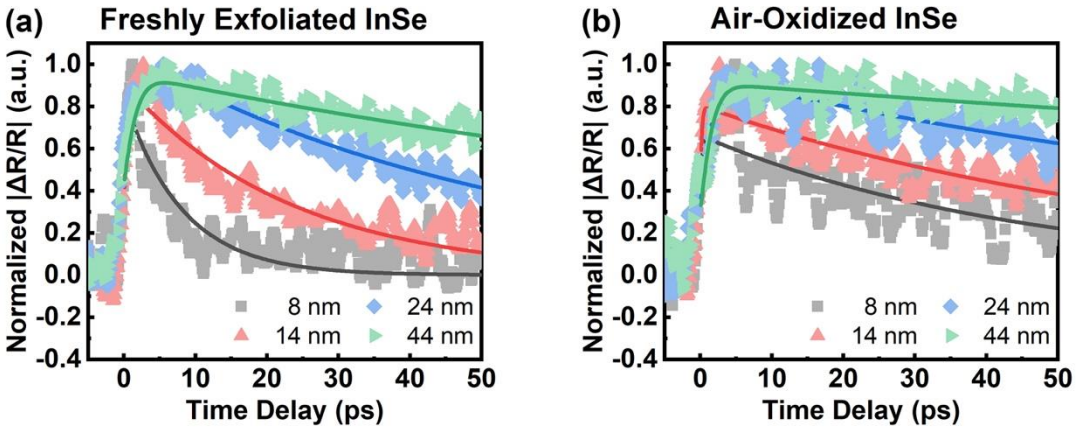


**Figure S6.** Thickness dependence on carrier recombination rate of InSe. The solid lines reveal the fitting curves based on a free carrier diffusion model to the experimental data shown in Fig. 3 in the main text.

## S9: Energy-dispersive X-ray spectroscopy (EDS) measurement

InSe flakes were mechanically exfoliated and transferred onto carbon tape for elemental analysis by EDS. A representative of EDS spectra for freshly exfoliated flake is shown in Fig. S7(a). The inset of Fig. S7(a) indicates the atomic percentage of Se element is slightly lower than that of In element. The detected carbon element should be from the carbon tape. After the samples were stored in ambient air (at 23°C) for over one month, oxygen element was detected on InSe as shown by the EDS spectra in Fig. S7(b). All samples on carbon tap identified by EDS were also measured by the pump-probe experiments. As shown in Fig. S7(c), the lifetime of air-oxidized sample is longer than that of freshly exfoliated one.

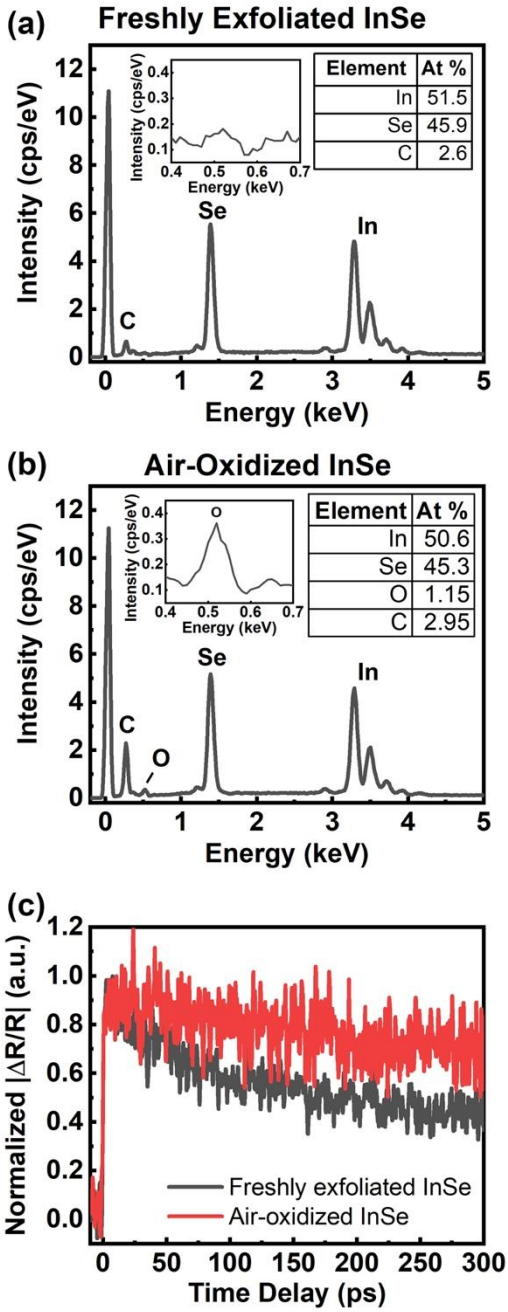


**Figure S7.** EDS analysis and normalized pump-probe curves of InSe on Carbon tape. EDS spectra of (a) freshly exfoliated and (b) air-oxidized samples. (c) Normalized pump-probe curves of the samples with and without identification of oxygen element by EDS.

## Reference


1 K. Nama Manjunatha and S. Paul, *Appl. Surf. Sci.*, 2015, **352**, 10-15.

2 J. Camassel, P. Merle, H. Mathieu and A. Chevy, *Phys. Rev. B*, 1978, **17**, 4718-4725.

3 Y. Yang, Y. Yan, M. Yang, S. Choi, K. Zhu, J. M. Luther and M. C. Beard, *Nat. Commun.*, 2015, **6**, 7961.

4 F. Ruf, Karlsruher Institut für Technologie (KIT), 2020.

5 M. V. Andriyashik, M. Yu. Sakhnovskii, V. B. Timofeev and A. S. Yakimova, *Phys. Stat. Sol. (b)*, 1968, **28**, 277-285.

6 C.-H. Ho and Y.-J. Chu, *Adv. Opt. Mater.*, 2015, **3**, 1750-1758.

7 K.-H. Lin, H.-Y. Cheng, C.-Y. Yang, H.-W. Li, C.-W. Chang and S.-W. Chu, *Appl. Phys. Lett.*, 2018, **113**, 171906.